Noise Propagation and Scaling in Regulation of Gonadotrope Biosynthesis

Frederique Ruf,*† Fernand Hayot,*† Myung-June Park,*† Yongchao Ge,*† Gang Lin,‡ Badrinath Roysam,‡ and Stuart C. Sealfon*†

*Department of Neurology and †Center for Translational Systems Biology, Mount Sinai School of Medicine, New York, New York; and ‡Department of Electrical, Computer, and Systems Engineering at Rensselaer Polytechnic Institute, Troy, New York

ABSTRACT Reproductive physiology depends on the control of biosynthesis in the pituitary gonadotrope by hypothalamic gonadotropin-releasing hormone (GnRH). The responses to GnRH include activation of extracellular signal-regulated kinase (ERK) and induction of Egr1. Using population and single cell signaling assays, we investigated the signal and noise transmission through this signaling and gene circuit, analyzing data obtained from 43,775 individual cells in 40 experiments. After exposure to GnRH, phosphorylated ERK (pERK) is elevated in 50% of the cells at 1.7 (SD = 0.3) min. Studies of the cell-to-cell response showed that for both pERK and for Egr1 protein production the mean response (μ) and standard deviation (σ) within individual cells were linearly related ($\sigma = k\mu$) and had similar values of k. To understand the basis for the scaling observed for noise propagation through this system, we determined the relationship between pERK and *egr1* mRNA levels induced at varying concentration of GnRH. While both pERK and *egr1* mRNA show a saturating sigmoidal relationship to the concentration of GnRH exposure, *egr1* mRNA is linearly related to the levels of pERK. These results explain the basis for variation in cellular responses in an important mammalian signaling pathway leading to gene induction.

INTRODUCTION

Mammalian reproduction depends on the reliable transmission of biosynthetic instructions from the brain hypothalamus to the pituitary gonadotrope. The hypothalamus secretes gonadotropin-releasing hormone (GnRH) that complexes with high affinity GnRH receptors on the gonadotrope membrane to regulate signaling and synthesis of the gonadotropins luteinizing hormone and follicle-stimulating hormone. The target gonadotropins are regulated downstream of a complex integrated signaling and gene network (1–3). Reproduction and survival of a mammalian species depends on the capacity of the gonadotrope to decode and respond appropriately to varying patterns of GnRH stimulation.

One key pathway in the gonadotrope's response to GnRH involves the activation of the mitogen-activated protein kinase extracellular signal-regulated kinase and subsequent induction of the transcription factor Egr1 (Fig. 1). This response system is necessary for mammalian reproduction; Egr1 is required for the synthesis of luteinizing hormone and the *egr1* null mouse is infertile (4,5). To understand the mechanisms underlying the decoding of biosynthetic instructions by the gonadotrope, we studied single cell responses in this pathway. We previously investigated the concentration-dependence of extracellular signal-regulated kinase (ERK) activation and Egr1 induction at the single cell level. We identified a mixed analog-digital response that may be advantageous by improving the overall reliability of gonadotrope responses to GnRH pulses that vary widely in amplitude (6).

Biochemical studies of cell signaling and gene induction performed on populations of cells have defined the connections that activate or repress responses and have elucidated the overall topology of the molecular networks. Biochemical studies of populations of cells, however, do not reveal the variations in individual cell responses. In most systems, the single cell represents the basic computational unit determining the response to stimuli. Therefore, it is important to investigate the propagation and control of signaling variation at the single cell level. Recent studies in unicellular organisms demonstrate a surprisingly high level of cell-to-cell variation in signaling responses (7–12). Few attempts have been made to characterize the mechanisms underlying response variation in more complex mammalian signaling networks. The propagation of variation through a signaling pathway and gene induction has not been assayed directly in previous studies. This study focuses on characterizing the time of signal transduction to the nucleus in individual synchronized cells derived from mammalian gonadotropes and on investigating the basis of cell-to-cell variation in responses.

EXPERIMENTAL PROCEDURES

Cell culture

LβT2 cells obtained from Prof. Pamela Mellon (University of California, San Diego, CA) were maintained at 37°C, 5% CO_2 in humidified air in phenol-red free DMEM (Mediatech, Herndon, VA) supplemented with 10% fetal bovine serum (FBS) (Gemini, Calabasas, CA) and L-glutamine (Gibco,

Submitted June 14, 2007, and accepted for publication August 8, 2007.

Address reprint requests to Stuart C. Sealfon, Tel: 212-241-7075, E-mail: stuart.sealfon@mssm.edu.

Myung-June Park's present address is Dept. of Chemical Engineering, Ajou University, Suwon 443-749, Korea.

Editor: Byron Goldstein.

0006-3495/07/12/4474/07 $2.00

doi: 10.1529/biophysj.107.115170

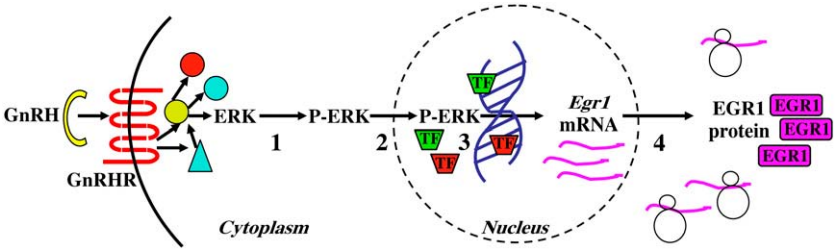

FIGURE 1 GnRH induction of Egr1 through ERK. We represented the major steps (1–4) between activation of the GnRH receptor by GnRH to the production of the Egr1 protein. 1: GnRH complexing to its receptor leads to ERK phosphorylation. 2: ERK translocates to the nucleus. 3: ERK activates preformed transcription factors and induces production of *egr1* mRNA. 4: *egr1* mRNA translocates to the cytoplasm where synthesis of Egr1 protein occurs.

Invitrogen, Carlsbad, CA). For immunohistochemical assays, 200,000 cells were seeded on poly-D-lysine (No. 7280; Sigma Aldrich, St. Louis, MO) pretreated glass coverslips (#1.5, 18 × 18 mm; Fisher Scientific, Pittsburgh, PA) in six-well plates. Cells were synchronized in 0.5% charcoal-treated FBS (CT-FBS; HyClone Laboratories, Logan, UT), L-glutamine, and 25 mM HEPES (Mediatech, Herndon, VA).

Antibodies

Antibodies used were phosphorylated ERK (pERK) antibody (#9106, Cell Signaling, Danvers, MA), total ERK antibody (#9102, Cell Signaling), Egr1 (sc-110, Santa Cruz Biotechnology, Santa Cruz, CA), and secondary Alexa 568-fluorophore coupled antibody (Invitrogen, Carlsbad, CA).

Immunohistochemistry

100 nM GnRH diluted in DMEM with 0.5% CT-FBS, L-glutamine and 25 mM HEPES was added for a specific time (as indicated on the figures) to synchronized cells maintained at 37°C either on a heat-pad for periods up to 5 min, or in the tissue-culture incubator for longer time points. The procedure followed is described in Ruf et al. (6). Briefly the cells were fixed in 4% formaldehyde (ultrapure EM grade; Polysciences, Warrington, PA) for 30 min at room temperature (RT), permeabilized in 0.2% triton/1× PBS (Triton, Sigma-Aldrich) for 10 min at RT, and quenched in 50 mM NH_4Cl (Sigma-Aldrich) for 5 min at RT, and blocked in phosphate buffered saline/0.1% Tween/5% BSA (Roche Diagnostics, Mannheim, Germany) for 1 h at RT. Anti-pERK antibody (1:1000) was added and incubated overnight at 4°C. Secondary 568 fluorophore-coupled antibody was added (1:1000) for 2 h, RT. After washing and 4',6'-diamidino-2-phenylindole counterstaining (DAPI, 0.1 μg/mL, Sigma-Aldrich), coverslips were mounted in Prolong Gold Antifade reagent (Invitrogen).

Fluorescent microscopy and data analysis

Fluorescent microscopy and data analysis was performed as described in Ruf et al. (6). Briefly, a Zeiss LSM510-META inverted confocal laser-scanning microscope was used for confocal imaging (Carl Zeiss, Oberkochen, Germany) and an Olympus BX-60 microscope coupled with a BX-FLA Reflected Light Fluorescence Attachment and a CCD-based image analysis system was used for epifluorescence imaging (Olympus, Melville, NY). Lasers and filters were set up for imaging Alexa-568 and DAPI. The exposure settings were determined empirically for each channel from control background and unchanged within an experiment. At least 10 images of nonoverlapping areas with 50–400 cells were assayed for each condition in each experiment.

Automated image quantification and data processing

Digital images were analyzed in a custom automated image analysis suite called 3D-CatFISH (13,14) as described in Ruf et al. (6). First, the cell nuclei were segmented using DAPI with the enhanced 3D watershed algorithm (15) followed by model-based object merging (16). Then, a desired region-of-interest was defined based on geometric distance for each segmented nucleus (i.e., a collar of five pixels), and specific signals were quantified in nucleus and cytoplasm. Each image was visually inspected for possible segmentation errors. The lowest individual fluorescence levels were used to normalize across coverslips within each experiment and analyzed in MatLab 7.0 (The MathWorks, Natick, MA) using the Savitzky-Golay function (17,18) and the curve-fitting toolbox.

ELISA assay

pERK and total ERK assay kits (KHO0091 and KHO0081; Biosource, Camarillo, CA) were used according to manufacturer's instructions. Briefly, the LβT2 cells were grown in six-well plates at 2.5 million cells/well and synchronized for cell-cycle in low serum for 24 h. After the treatment, cells were washed, lysed in cell extraction buffer (FN0011, Biosource), boiled and diluted (1:10) into the assay buffer provided by the manufacturer. Each sample was divided into two wells for assay of total and pERK.

Quantitative real-time PCR (qPCR)

For qPCR experiments, cells were seeded in 12-well plates at 750,000 cells per well. The medium was replaced 24 h later with DMEM containing 25 mM HEPES (Mediatech), 0.5% CT-FBS (HyClone Laboratories), and glutamine. On the next day, the cells were treated with the indicated concentrations of GnRH or vehicle and were returned to the CO_2 incubator for 40 min, at which point the medium was replaced with 360 μl lysis buffer (4 M guanidinium thiocyanate, 25 mM sodium citrate (pH 7.0), 0.5% N-lauroyl-sarcosine, and 0.1 M 2-mercaptoethanol). RNA was isolated according to the method of Chomczynski and Sacchi (19). Total RNA was isolated with the StrataPrep96 kit (Stratagene, La Jolla, CA). After reverse-transcription of 1 μg of RNA, the samples were diluted 1:20 in dH_2O. Later, SYBR green qPCR assays were performed (40 cycles) using 5 μl of cDNA template and 5 μl of master mix containing the specific primers for the targeted gene (*egr1* or *RPS11*) and the required qPCR buffers. The results were exported as Ct values for subsequent analysis. Three biological replicates were done. From the three-replicates measures of each biological sample, the mean, standard deviation and fold-changes to vehicle treatment were estimated and normalized to *RPS11*. The relative copy number of cDNA per assay was determined by running a standard curve with the PCR product for the specific gene. Results are presented as percentage of maximum.

RESULTS AND DISCUSSION

Temporal dynamics of pERK production after GnRH exposure

To select the time points for single cell studies, we first quantified the average time course for the early production of pERK after GnRH exposure. LβT2 gonadotrope cells were synchronized for cell cycle and exposed to 100 nM GnRH. pERK and total ERK levels were quantified by ELISA. After

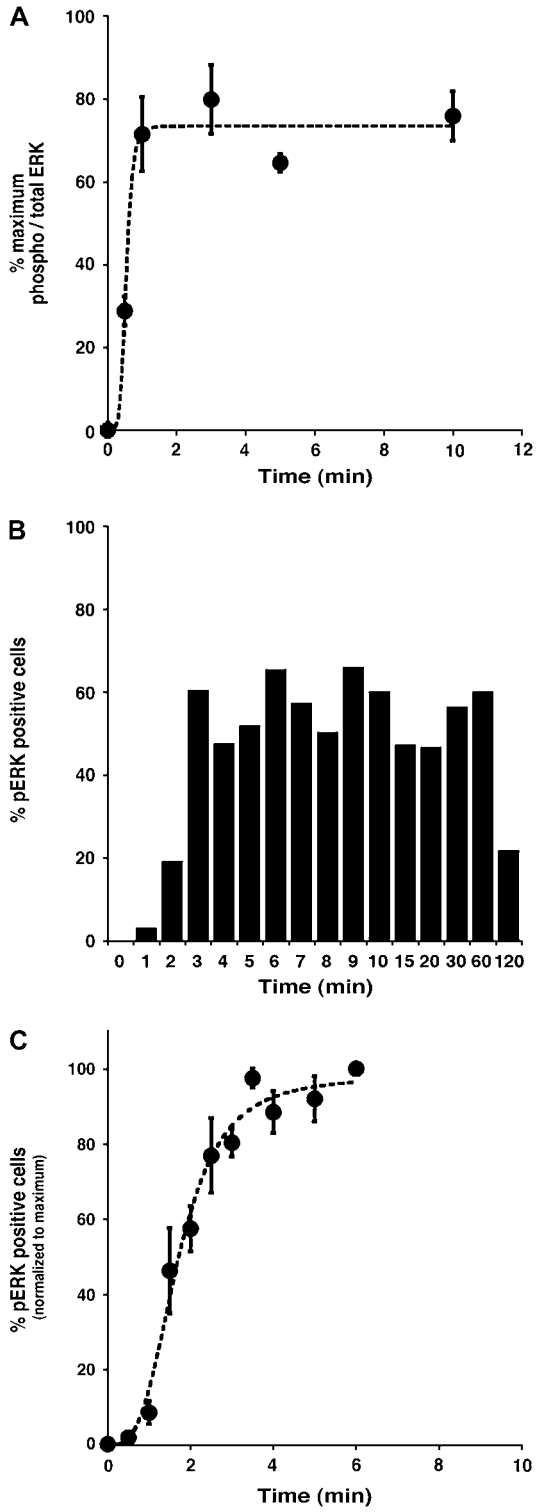

FIGURE 2 Quantification of nuclear ERK detection in average and single LβT2 gonadotropes. (*A*) LβT2 cells were treated with 100 nM GnRH for the indicated times. pERK and total ERK levels were quantified from whole-cell lysates by ELISA. Each point represents three individual cell samples, and error bars are standard errors. (*B*) Time-course of individual cell activation from 0 to 2 h. Cells were treated with 100 nM GnRH for the indicated times, processed for pERK immunohistochemistry and analyzed by automated analysis. The percentage of activated cells over time is represented. (*C*) Time-course of individual cell activation from 0 to 5 min from 12 independent experiments (see Supplementary Material Table 1). Cells were treated as described in panel *B*. Error bars are standard errors.

GnRH exposure, ERK is rapidly phosphorylated, with maximal levels of activation achieved and stable after ~2 min of GnRH exposure (Fig. 2 *A*). Between 0 and 2 min we detected intermediate levels of pERK.

Time delay of ERK induction in single gonadotrope cells suggests a rapid nuclear accumulation of pERK after GnRH exposure

We next studied the early nuclear localization of pERK after GnRH exposure in individual synchronized LβT2 gonadotrope cells (Fig. 2, *B* and *C*). These assays rely on immunohistochemistry using an antibody specific for doubly phosphorylated ERK combined with microscopy and automated image segmentation and analysis (6,13) (Fig. 3). Synchronization, viability, and image analysis controls that confirm the cell cycle arrest by p21 immunohistochemistry and validate the accuracy and reproducibility of this assay have been described previously (6).

The fraction of cells showing an increase in nuclear pERK increased rapidly during the first 3 min of GnRH exposure (Fig. 2, *B* and *C*, and Fig. 3). After this initial increase, the proportion of cells showing elevated nuclear pERK plateaus for the first hour of treatment (Fig. 2 *B*). The time-course of nuclear localization observed was similar in 12 separate experiments (Fig. 2 *C*, Supplementary Material Table 1). Fifty-percent of the cells show an elevated nuclear pERK 1.7 min (SD = 0.3) after GnRH exposure.

The time course observed for the average levels of pERK measured by ELISA (Fig. 2 *A*) and the fraction of individual cells showing increased nuclear pERK (Fig. 2, *B* and *C*) showed a close correspondence. Analysis of the level of nuclear pERK in individual cells was consistent with the presence of two populations of cells at all time points, cells showing a basal response and cells showing an elevated response (Fig. 3).

Scaling of cell-to-cell variations in nuclear pERK levels after GnRH stimulation of individual synchronized gonadotrope cells

Despite synchronization of the cells, the single cell results obtained showed very large cell-to-cell variations in the levels of nuclear pERK at steady state after 2 min of GnRH exposure (Fig. 4). Such wide variations in single cell responses are likely to have an important effect on the stimulus-response behavior of the entire hypothalamic-pituitary-gonadal axis. The characterization of cell-to-cell response variations or noise in unicellular organisms has recently become an important area of experimental and

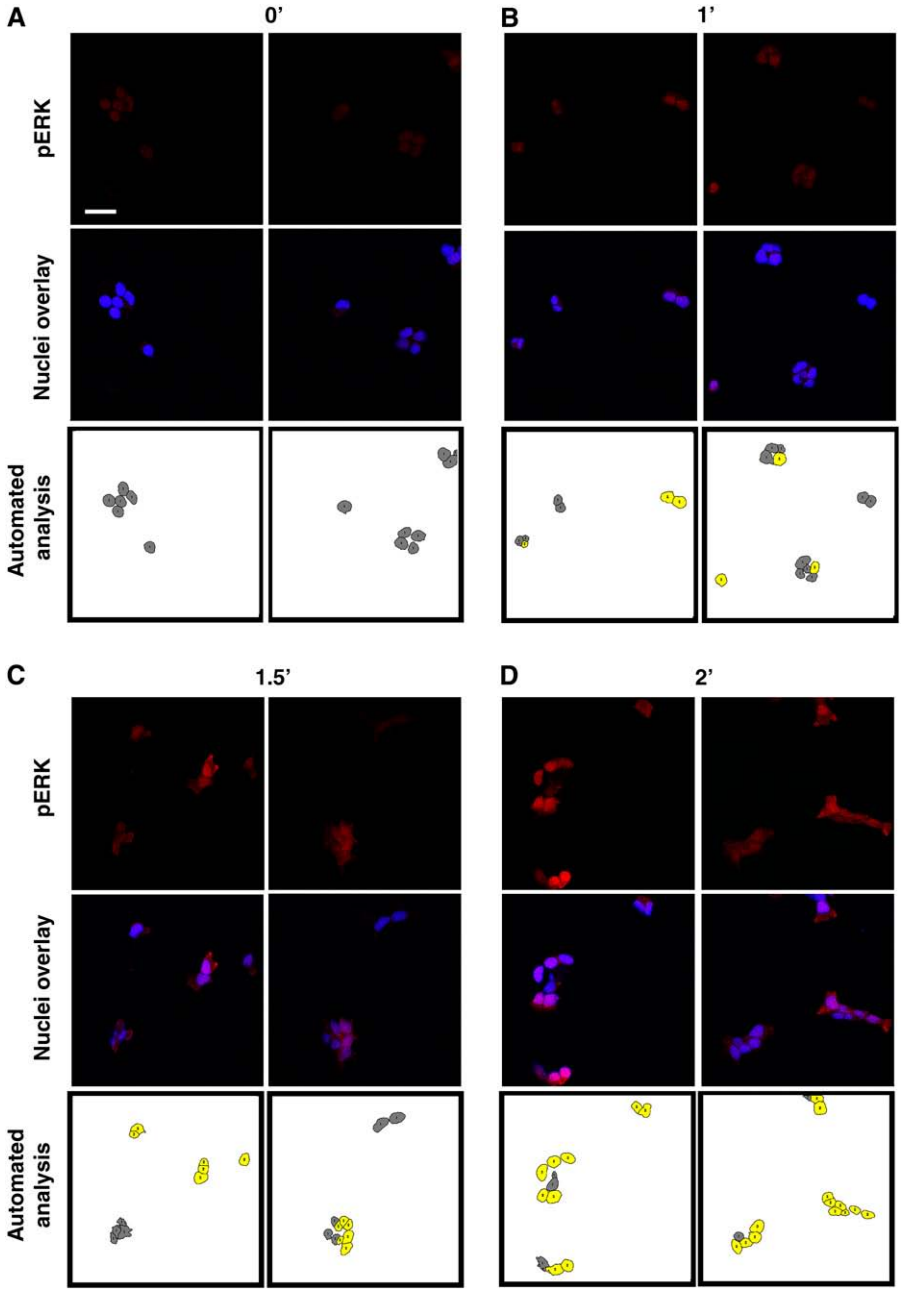

FIGURE 3 Photomicrographs and analysis of ERK phosphorylation in gonadotrope cells. LβT2 cells were treated with 100 nM GnRH for the indicated times (*A–D*). Two nonoverlapping representative photomicrographs are presented at each time point. (*Top*) pERK was detected using immunohistochemistry with an antibody-specific for doubly phosphorylated ERK (*red*). (*Middle*) Merged pictures with nuclear visualization using DAPI (*blue*), pERK (*red*). (*Bottom*) We used automated image analysis to identify activated from nonactivated cells. The threshold was set based on the basal level within cells of the 0 min images (*A*). Cells above threshold are marked in yellow, while nonactivated cells remain in gray. Scale bar = 20 μm.

theoretical research (reviewed in (20)). Cellular response variation has not been well-characterized in more complex, physiologically relevant systems. The induction of Egr1 in the gonadotrope by GnRH regulation of ERK represents a phosphorylation cascade and gene induction response of high physiological significance. The responses can be assayed directly at the single cell level at multiple loci in the response (see Fig. 1 in (6)). Therefore, we investigated the noise transmission through the gonadotrope at the level of both nuclear pERK and the subsequent synthesis of Egr1.

To assess the relationship of the variation in response among different cells to the average level of response, 40 experiments performed at different time points and different concentrations of GnRH were analyzed. Some of the primary data used in this analysis were reported previously (6) (see Supplementary Material Table 1 for time-course data and Supplementary Material Table 2 for concentration response data). We find that for both nuclear pERK and for Egr1 stimulated by GnRH the response variation (σ = SD) varies linearly with the average response (μ, Fig. 5, *A* and *B*). In addition, the coefficient of variation observed ($c.v. = \sigma/\mu$) was comparably $\sim$0.5 for both the nuclear localization of pERK and the downstream production of Egr1.

The noise observed did not result from either measurement variation or from differences in size of the nucleus. The variations in pERK and Egr1 observed were an

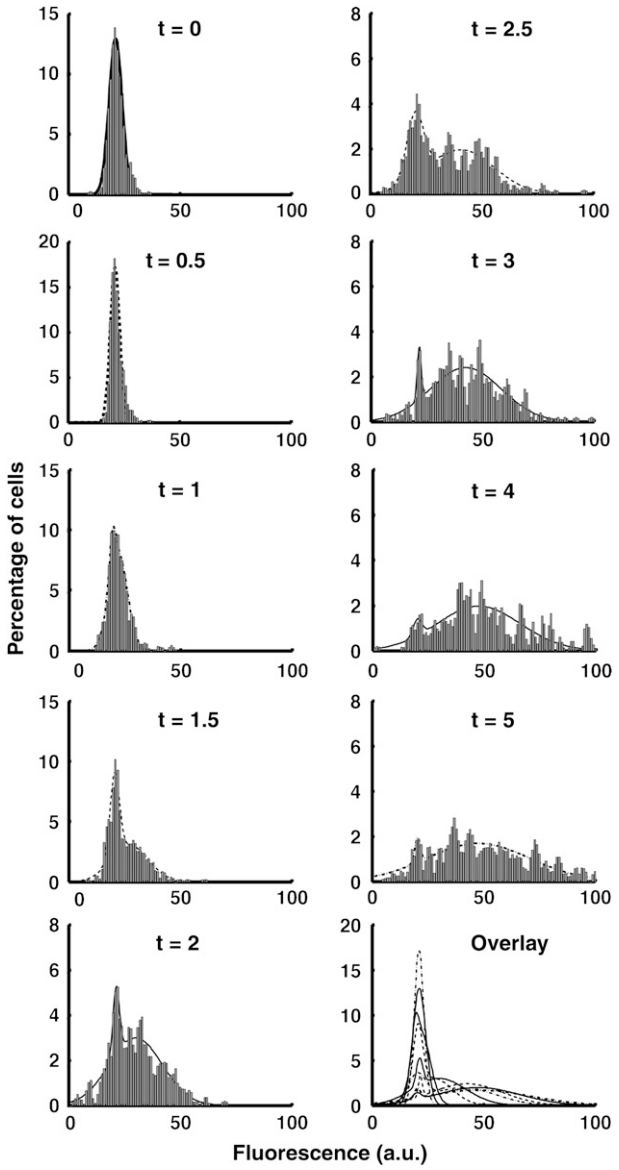

FIGURE 4 Distributions of single-cell pERK responses over time. The percentage of cells at different fluorescence levels (arbitrary units, a.u.) is shown for the different exposures with GnRH (representative experiment). The curve fitting was performed with two Gaussian distributions using MatLab.

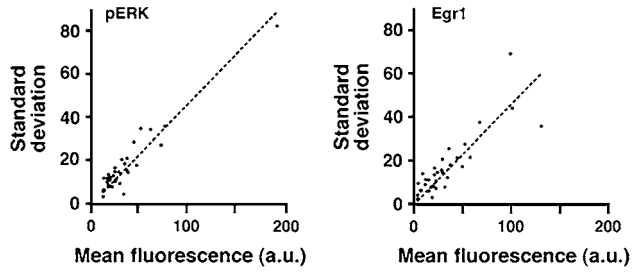

FIGURE 5 Analysis of cell-to-cell variations at two steps in the GnRH cascade. Cell-cell variations were analyzed based on concentration-response experiments at the level of pERK (*A*) and Egr1 protein (*B*) (6). *X* axis, mean fluorescence of the activated cells (arbitrary units, a.u.), *y* axis: standard deviation of individual cell fluorescence. The *R* square and slope are, respectively, 0.94; 0.465 (*A*, pERK) and 0.83; 0.461 (*B*, Egr1).

order-of-magnitude larger than the measurement error obtained when measuring spotted fluorophore (c.v. = 0.02; (6)). The individual gonadotropes show large variations in the size of their nucleus (Supplementary Material Fig. 1). However, quantification and analysis of pERK levels in individual cells as a function of nuclear size did not show any correlation (Supplementary Material Fig. 1).

The findings that the total noise expressed as standard deviation (σ scales directly in proportion to the average level of response) and that the c.v. is similar before and after gene transcription were initially surprising. If the cell-to-cell variability were dominated by a sequential birth-death process of protein and mRNA, the prediction based on this generalized Poisson process would be that the variance (σ^2), not the standard deviation, should scale as the mean level of expression (σ^2 proportional to μ) (7,10). Two studies have investigated the scaling of noise in yeast using flow cytometry and GFP tagging of a large number of proteins. Both studies have found that when studying the cell-to-cell variation of a large number of proteins, an overall pattern of σ^2 proportional to μ is observed (7,10). However, a different study in yeast measuring the output of the α-mating factor signaling pathway using a reporter construct found a constant c.v. (σ proportional to μ) (8), consonant with our results.

We suspected that there were two different processes contributing to cell-to-cell expression variation. The birth-death process of genes and proteins has a scaling of σ^2 proportional to μ. Regulated proteins and genes have a second, potentially larger source of variation arising from cell-to-cell variation in the capacity of the signaling pathway in each cell to generate a response to an identical stimulus (8). An example of one potential cause for such a pathway response variation is differences in the single cell level of the GnRH receptor. Chemical inactivation studies have shown that the signaling response to GnRH depends on the level of receptor expression (21). A recent study in transfected cells showed that the levels of nuclear accumulation of a pERK-GFP reporter depended on the level of receptor expression (22).

For simplicity, we assume that the single cell pERK response is proportional to the pathway capacity of that cell, *R*, and that pathway capacity is normally distributed.

The response in each cell can be expressed as

$$pERK = R * f(GnRH),$$
$$\mu = \langle pERK \rangle = \langle R \rangle * f(GnRH),$$
$$\sigma^2 = \sigma_R^2 * f(GnRH)^2,$$

where $\langle \ldots \rangle$ indicate the average, $f(GnRH)$ is the function relating input GnRH concentration to response, σ^2 is the

variance in pERK due to differences in pathway capacity, and σ_R^2 is the variance of the pathway capacity. This gives σ proportional to μ.

Total variance is the sum of the pathway noise (σ^2) and the variance arising from the presumably independent generalized Poisson process. The contribution of Poisson process noise to σ/μ is proportionally greater at lower levels of μ. As our data show no loss of linearity comparing σ to μ at low concentrations (Fig. 5), the relative contribution of a generalized Poisson process (σ^2 to μ) to cell-to-cell response variations in pERK activation and Egr1 synthesis appears to be slight. This formulation suggests that when the noise of regulated responses such as ERK activation or *egr1* induction are measured and compared with each other under varied input conditions then the σ proportional to μ-noise will dominate, whereas σ^2 proportional to μ would be most apparent when comparing steady state levels of different genes or proteins. Thus a study and analysis of single responses such as ours or the yeast study of Colman-Lerner et. al. (8) would be described better as the σ/μ pathway type of variation, and studies comparing many proteins (7,10) would see a predominance of the σ^2/μ Poisson process type of noise. We tested this by examining the σ and μ relationship observed when analyzing the noise for each protein individually using the primary data from a published yeast study that reported an overall cell-to-cell variation that scales as a Poisson process, σ^2 to μ (7,10) (kindly provided by Prof. N. Barkai, Weizmann Institute). When single cell data obtained under varied conditions for each protein were analyzed separately, for a number of the genes the data were best fit as σ proportional to μ (analysis not shown). These observations are consistent with our hypothesis and reconcile the differences in noise scaling reported in different studies.

Another aspect of our results that required further inquiry was the basis for the similar c.v. observed at the level of pERK and Egr1. This relationship implies that the variation arose earlier in the signaling system and that the responses between pERK and gene induction are working merely as linear multipliers. Biochemical signaling and enzymatic reactions are saturable and are usually well represented by a Hill function. However, the noise propagation we observed suggests that the biochemical processes between ERK and gene activation were all functioning at stimulus levels making them nearly linear functions.

This analysis led us to test the function relating pERK to the activation of the *egr1* gene by performing detailed concentration response studies. Both pERK and *egr1* are well described by a Hill function acting on the concentration of GnRH (Fig. 6, *A* and *B*). As predicted, however, *egr1* is linearly related to the concentration of pERK (Fig. 6 *C*). This linearity suggests that the reactions between ERK activation and gene induction do not saturate and appears to explain the pattern of noise propagation observed in this study.

Recent studies investigating single cell responses demonstrate a strikingly high level of signaling and gene induction noise (7–12). In a previous study, we showed that the response to varying levels of GnRH in the gonadotrope has been engineered to have a mixed analog-digital response, a design that may provide some benefits in improving the reliability of responses to the varying pulse concentrations of GnRH secreted by the brain (6). This study shows the temporally synchronized rapid nuclear localization of pERK and clarifies the scaling properties of noise in regulated molecular networks. The cell-to-cell variations in pERK nuclear accumulation and Egr1 induction show that the standard deviation is similarly proportional to the mean response at the level of the pathway and the downstream gene induction. The mechanisms utilized to maintain this relatively constant variation in this integrating signaling and biosynthetic pathway remains to be discovered. Elucidating the role and control of signaling noise is central to understanding the function and dysfunction of the reproductive axis.

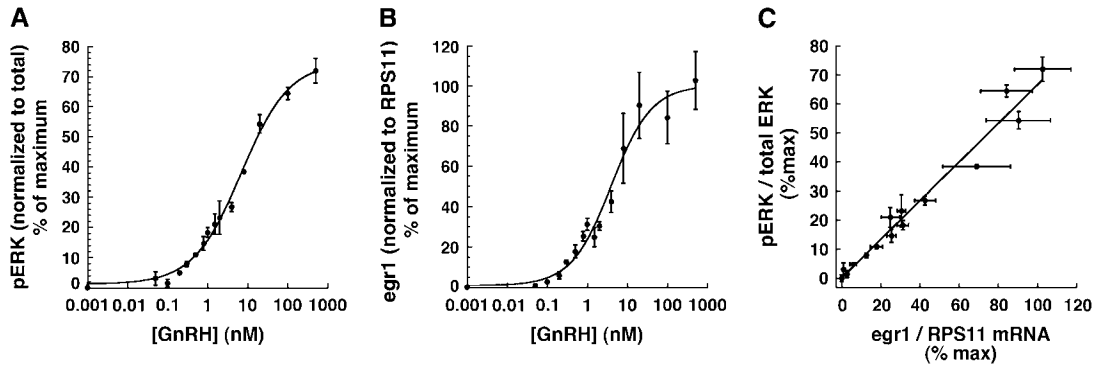

FIGURE 6 Linearity between pERK and *egr1* mRNA. (*A*) Concentration response curve for average pERK (normalized to total ERK, and presented as percentages of maximum) obtained by ELISA with each point representing three independent whole-cell lysates obtained at the specific GnRH concentration (*x* axis) after 35 min of treatment, and error bars as standard deviations. (*B*) Concentration response curve for average *egr1* mRNA (normalized to *RPS11* mRNA, and presented as percentages of maximum) obtained by quantitative real-time PCR with each point representing three independent whole-cell lysates obtained at the specific GnRH concentration (*x* axis) after 35 min of treatment, and error bars as standard deviations. (*C*) Linearity between pERK and *egr1* mRNA. For each GnRH concentration, the responses at each level were plotted and fitted with a linear regression. Error bars are standard deviations.

SUPPLEMENTARY MATERIAL

To view all of the supplemental files associated with this article, visit www.biophysj.org.

We thank Dr. Naama Barkai for graciously providing the primary data from her publication, Dr. Robert Pfeffer for discussions and helpful comments, Dr. Pamela Mellon for providing the LβT2 cells, and the Mount Sinai Real Time PCR and Microscopy Shared Research Facilities for instrumentation and assistance.

This research was supported by National Institutes of Health grant No. DK46943.

REFERENCES

1. Ruf, F., M. Y. Fink, and S. C. Sealfon. 2003. Structure of the GnRH receptor-stimulated signaling network: insights from genomics. *Front. Neuroendocrinol.* 24:181–199.
2. Ruf, F., and S. C. Sealfon. 2004. Genomics view of gonadotrope signaling circuits. *Trends Endocrinol. Metab.* 15:331–338.
3. Wurmbach, E., T. Yuen, B. J. Ebersole, and S. C. Sealfon. 2001. Gonadotropin-releasing hormone receptor-coupled gene network organization. *J. Biol. Chem.* 276:47195–47201.
4. Lee, S. L., Y. Sadovsky, A. H. Swirnoff, J. A. Polish, P. Goda, G. Gavrilina, and J. Milbrandt. 1996. Luteinizing hormone deficiency and female infertility in mice lacking the transcription factor NGFI-A (Egr-1). *Science.* 273:1219–1221.
5. Topilko, P., G. Levi, G. Merlo, S. Mantero, C. Desmarquet, G. Mancardi, and P. Charnay. 1997. Differential regulation of the zinc finger genes Krox-20 and Krox-24 (Egr-1) suggests antagonistic roles in Schwann cells. *J. Neurosci. Res.* 50:702–712.
6. Ruf, F., M. J. Park, F. Hayot, G. Lin, B. Roysam, Y. Ge, and S. C. Sealfon. 2006. Mixed analog/digital gonadotrope biosynthetic response to gonadotropin-releasing hormone. *J. Biol. Chem.* 281:30967–30978.
7. Bar-Even, A., J. Paulsson, N. Maheshri, M. Carmi, E. O'Shea, Y. Pilpel, and N. Barkai. 2006. Noise in protein expression scales with natural protein abundance. *Nat. Genet.* 38:636–643.
8. Colman-Lerner, A., A. Gordon, E. Serra, T. Chin, O. Resnekov, D. Endy, C. G. Pesce, and R. Brent. 2005. Regulated cell-to-cell variation in a cell-fate decision system. *Nature.* 437:699–706.
9. Elowitz, M. B., A. J. Levine, E. D. Siggia, and P. S. Swain. 2002. Stochastic gene expression in a single cell. *Science.* 297:1183–1186.
10. Newman, J. R., S. Ghaemmaghami, J. Ihmels, D. K. Breslow, M. Noble, J. L. DeRisi, and J. S. Weissman. 2006. Single-cell proteomic analysis of *S. cerevisiae* reveals the architecture of biological noise. *Nature.* 441:840–846.
11. Ozbudak, E. M., M. Thattai, I. Kurtser, A. D. Grossman, and A. van Oudenaarden. 2002. Regulation of noise in the expression of a single gene. *Nat. Genet.* 31:69–73.
12. Raser, J. M., and E. K. O'Shea. 2004. Control of stochasticity in eukaryotic gene expression. *Science.* 304:1811–1814.
13. Chawla, M. K., G. Lin, K. Olson, A. Vazdarjanova, S. N. Burke, B. L. McNaughton, P. F. Worley, J. F. Guzowski, B. Roysam, and C. A. Barnes. 2004. 3D-catFISH: a system for automated quantitative three-dimensional compartmental analysis of temporal gene transcription activity imaged by fluorescence in situ hybridization. *J. Neurosci. Methods.* 139:13–24.
14. Lin, G., M. K. Chawla, K. Olson, J. F. Guzowski, C. A. Barnes, and B. Roysam. 2005. Hierarchical, model-based merging of multiple fragments for improved three-dimensional segmentation of nuclei. *Cytometry A.* 63:20–33.
15. Lin, G., U. Adiga, K. Olson, J. F. Guzowski, C. A. Barnes, and B. Roysam. 2003. A hybrid 3D watershed algorithm incorporating gradient cues and object models for automatic segmentation of nuclei in confocal image stacks. *Cytometry A.* 56:23–36.
16. Lin, G., C. V. Stewart, B. Roysam, K. Fritzsche, G. Yang, and H. L. Tanenbaum. 2004. Predictive scheduling algorithms for real-time feature extraction and spatial referencing: application to retinal image sequences. *IEEE Trans. Biomed. Eng.* 51:115–125.
17. Madden, H. 1978. Comments on the Savitzky-Golay convolution method for least-squares fit smoothing and differentiation of digital data. *Anal. Chem.* 50:1383–1386.
18. Savitzky, A., and M. J. E. Golay. 1964. Smoothing and differentiation of data by simplified least squares procedures. *Anal. Chem.* 36: 1627–1639.
19. Chomczynski, P., and N. Sacchi. 1987. Single-step method of RNA isolation by acid guanidinium thiocyanate-phenol-chloroform extraction. *Anal. Biochem.* 162:156–159.
20. Maheshri, N., and K. E. O'Shea. 2007. Living with noisy genes: how cells function reliably with inherent variability in gene expression. *Annu. Rev. Biophys. Biomol. Struct.* 36:413–434.
21. Zhou, W., V. Rodic, S. Kitanovic, C. A. Flanagan, L. Chi, H. Weinstein, S. Maayani, R. P. Millar, and S. C. Sealfon. 1995. A locus of the gonadotropin-releasing hormone receptor that differentiates agonist and antagonist binding sites. *J. Biol. Chem.* 270:18853–18857.
22. Caunt, C. J., A. R. Finch, K. R. Sedgley, L. Oakley, L. M. Luttrell, and C. A. McArdle. 2006. Arrestin-mediated ERK activation by gonadotropin-releasing hormone receptors: receptor-specific activation mechanisms and compartmentalization. *J. Biol. Chem.* 281: 2701–2710.